PNAS RESEARCH ARTICLE | MICROBIOLOGY

# Polyamines and linear DNA mediate bacterial threat assessment of bacteriophage infection

Camilla D. de Mattos[a,1], Dominick R. Faith[a,1], Artem A. Nemudryi[b], Amelia K. Schmidt[a], DeAnna C. Bublitz[a], Lauren Hammond[c], Margie A. Kinnersley[a], Caleb M. Schwartzkopf[a], Autumn J. Robinson[a], Alex Joyce[a], Lia A. Michaels[a], Robert S. Brzozowski[a], Alison Coluccio[a], Denghui David Xing[a], Jumpei Uchiyama[d], Laura K. Jennings[a], Prahathees Eswara[c], Blake Wiedenheft[b], and Patrick R. Secor[a,2]

Edited by Christine Jacobs-Wagner, Stanford University, Stanford, CA; received September 27, 2022; accepted January 10, 2023

**Monitoring the extracellular environment for danger signals is a critical aspect of cellular survival. However, the danger signals released by dying bacteria and the mechanisms bacteria use for threat assessment remain largely unexplored. Here, we show that lysis of *Pseudomonas aeruginosa* cells releases polyamines that are subsequently taken up by surviving cells via a mechanism that relies on Gac/Rsm signaling. While intracellular polyamines spike in surviving cells, the duration of this spike varies according to the infection status of the cell. In bacteriophage-infected cells, intracellular polyamines are maintained at high levels, which inhibits replication of the bacteriophage genome. Many bacteriophages package linear DNA genomes and linear DNA is sufficient to trigger intracellular polyamine accumulation, suggesting that linear DNA is sensed as a second danger signal. Collectively, these results demonstrate how polyamines released by dying cells together with linear DNA allow *P. aeruginosa* to make threat assessments of cellular injury.**

bacteriophage | *Pseudomonas aeruginosa* | danger sensing | phage defense | polyamine

## Significance

When cells lyse, danger signals are released into the environment that warn adjacent cells of nearby danger. However, the molecules that serve as bacterial danger signals are poorly defined, and how danger signals affect bacterial responses to threats such as bacteriophage infection are unknown. Here, we demonstrate that polyamines released by lysed bacteria are internalized by adjacent cells. In the absence of bacteriophage infection, intracellular polyamine levels quickly return to baseline. When bacteriophage infect a cell, they inject linear DNA that causes intracellular polyamine levels to remain high, interfering with bacteriophage DNA replication. Our results indicate that polyamines released by lysed cells and linear DNA associated with bacteriophage infection are danger signals that guide bacterial threat assessment of bacteriophage infection.

Endogenous danger signals are passively released upon cellular injury caused by mechanical damage or infection by pathogens. In eukaryotic cells, molecules such as adenosine triphosphate (ATP), intracellular proteins, oxidized lipids, and others, serve as danger signals that are sensed by conserved pattern recognition receptors (PRRs) on neighboring cells (1–4). PRRs also detect microbial-derived molecules and stimulate antimicrobial immune responses (5). Eukaryotic cells take cues from both damage- and microbial-derived molecules to make threat assessments of cellular injury (2).

Bacteria also sense and respond to molecules released by lysed bacteria (6–9). For example, the pathogen *Pseudomonas aeruginosa* can detect molecules released by lysed bacteria via the Gac/Rsm pathway (7). In response to kin cell lysis, Gac/Rsm up-regulates antibacterial pathways that protect *P. aeruginosa* from competing bacterial species. However, the molecules that serve as danger signals in bacteria are poorly characterized and how they influence bacterial responses to viral (phage) infection remains largely unexplored.

In this study, we test the hypothesis that lysed bacterial cells release danger signals that induce phage-resistance phenotypes in surviving cells. We use RNA sequencing and microbial genetics to characterize cellular responses of *P. aeruginosa* to kin cell lysates and phage infection. We identify both polyamines and linear DNA as danger signals that guide bacterial responses to cellular injury. High concentrations of extracellular polyamines cause intracellular polyamine levels to spike. In uninfected cells, intracellular polyamines are catabolized and return to basal levels. In phage-infected cells, intracellular polyamines levels increase and remain elevated, which inhibits phage nucleic acid replication. Many phage species inject linear DNA into bacterial cells and linear DNA is sufficient to trigger intracellular polyamine accumulation. Finally, Gac/Rsm signaling is required for *P. aeruginosa* to increase and maintain high intracellular polyamine levels, indicating a major role for Gac/Rsm signaling in regulating intracellular polyamine homeostasis. Because polyamines are ubiquitous and Gac/Rsm signaling is conserved across γ-proteobacteria, intracellular polyamine accumulation may be a general strategy employed by bacteria to defend against phage infection.

## Results

**A Small Water-Soluble Molecule Released by Lysed Bacteria Suppresses Phage Replication.** Since phage infections can result in mass bacterial cell lysis, we hypothesized that signals released by lysed bacteria would suppress phage replication in nearby cells. To test this hypothesis, we generated *P. aeruginosa* lysates from infected and uninfected cells.

Author contributions: P.R.S. designed research; C.D.d.M., D.R.F., A.K.S., D.C.B., L.H., M.A.K., C.M.S., A.J.R., A.J., L.A.M., R.S.B., A.C., D.D.X., L.K.J., P.E., and P.R.S. performed research; J.U. contributed new reagents/analytic tools; C.D.d.M., D.R.F., A.A.N., A.K.S., D.C.B., L.H., M.A.K., P.E., B.W., and P.R.S. analyzed data; and B.W. and P.R.S. wrote the paper.

The authors declare no competing interest.

This article is a PNAS Direct Submission.



[1]C.D.d.M. and D.R.F. contributed equally to this work.

[2]To whom correspondence may be addressed. Email: Patrick.secor@mso.umt.edu.

This article contains supporting information online at https://www.pnas.org/lookup/suppl/doi:10.1073/pnas.2216430120/-/DCSupplemental.

Published February 21, 2023.

After removing cell debris by centrifugation and virions by filtration through a 100-kDa membrane (*SI Appendix*, Fig. S1*A*), lysates were used to make LB-lysate agar plates. Lawns of *P. aeruginosa* PAO1 grown on lysogeny broth (LB) agar or LB-lysate agar were then challenged with phage species representing major diverse groups Siphoviridae (JBD26, DMS3vir), Podoviridae (CMS1), Myoviridae (F8), and Inoviridae (Pf4).

Replication of all phages except CMS1 was inhibited on LB-lysate agar derived from phage lysate (Fig. 1*A*). A similar phage-resistant phenotype is also evident on LB-lysate agar plates derived from cells lysed by sonication (Fig. 1*B*), indicating that phage infection is not a prerequisite for induction of a lysate-induced phage-resistant phenotype. When *P. aeruginosa* collected from LB-lysate agar were replated onto LB agar, sensitivity to phage infection is restored (Fig. 1*B*), indicating that cell lysates induce transient phage-resistance in *P. aeruginosa* rather than heritable mutations that confer phage resistance.

We hypothesized that the cell lysates contain a danger signal that induces phage resistance. To determine if the molecule(s) responsible for inducing phage resistance are hydrophobic or water-soluble, we extracted LB lysate (derived from sonicated cells) with chloroform ($CHCl_3$) and used the aqueous phase to make agar plates. We repeated the plaque assays using the well-characterized virulent mutant of DMS3 (DMS3vir) (10). This experiment demonstrates that the active molecule(s) are retained in the aqueous phase, pass through a 3 kDa molecular weight cutoff membrane, and retain antiphage activity after lyophilization and rehydration (Fig. 1*C*). Together, these results indicate that small water-soluble molecule(s) induce a transient phage resistance phenotype in *P. aeruginosa*.

**Polyamines Induce Phage Resistance in *P. aeruginosa*.** To aid in identifying the signal in cell lysate that induces phage resistance, we used RNA-seq to determine how LB-lysate agar affected the transcriptional profile of *P. aeruginosa*. In *P. aeruginosa* growing on LB-lysate agar, 394 genes were differentially regulated compared with cells growing on LB agar (Fig. 2*A* and Dataset S1, PRJNA806967) (11). Gene enrichment analysis revealed that spermidine and polyamine catabolism (breakdown) genes are up-regulated and overrepresented in LB-lysate agar datasets (Fig. 2*B*), some of which are highlighted in the volcano plot in Fig. 2*A*.

In bacteria, putrescine and spermidine (Fig. 2*C*) are the most common polyamines (12) and are typically present inside bacterial cells at concentrations ranging from 0.1 to 30 mM (13, 14). We tested whether millimolar concentrations of polyamine could be released into the local environment in response to phage infection or other mass-lysis events. Indeed, in the cell lysates we used to make LB-lysate agar plates, total polyamine concentrations were approximately 30 mM (Fig. 2*D*). Furthermore, DMS3vir triggered cell lysis 4 to 6 h postinfection (Fig. 2*E*), releasing ~20 mM total polyamine (Fig. 2*F*). When exogenous polyamine concentrations were normalized to bacterial density ($OD_{600}$), a dramatic increase in polyamine release was observed 4 to 6 h postinfection (Fig. 2*G*), indicating that phage-induced lysis of *P. aeruginosa* releases abundant polyamines into the environment.

To test the hypothesis that polyamines inhibit the phage lifecycle, we grew *P. aeruginosa* lawns on LB agar (3-(N-morpholino) propanesulfonic acid (MOPS) buffered at pH 7.2) supplemented with 0 to 100-mM of commercially available putrescine, spermidine, or spermine. All polyamines suppressed DMS3vir replication in a dose-dependent manner (Fig. 2 *H–J*) with putrescine significantly ($P < 0.05$) inhibiting DMS3vir replication at concentrations as low as 0.1 mM (*SI Appendix*, Fig. S2 *A* and *B*). Putrescine also inhibited replication of phages Pf4, JBD26, and F8, but not CMS1 (Fig. 2 *J* and *K*), consistent with our observations using crude bacterial lysates (Fig. 1 *A* and *B*). In addition to polyamines, we also tested ornithine, which is a precursor to polyamines (15). Ornithine concentrations as high as 100 mM do not affect phage replication (*SI Appendix*, Fig. S2 *C* and *D*) indicating that polyamine precursor availability does not influence phage resistance. Collectively, these results indicate that polyamines are the signal in cell lysates that induce phage resistance.

**Polyamines and Phage Infection Synergize to Up-Regulate Phage Defense Systems in *P. aeruginosa*.** We hypothesized that if polyamines are perceived as a danger signal, they might activate endogenous phage defense systems. We examined phage defense gene expression in our RNAseq data. We used DefenseFinder (16) and Prokaryotic Antiviral Defence LOCator (PADLOC) (17) to identify four putative phage defense systems encoded by *P. aeruginosa* PAO1: i) a retron, ii) a toxin/antitoxin pair, iii) a Gabija system, and iv) a type I restriction modification system.

Polyamines and phage infection together synergistically and significantly up-regulate all four putative phage defense systems (*SI Appendix*, Fig. S3 and Table S1). In contrast, compared with cells grown in LB broth, putrescine alone down-regulated phage defense transcription, although this was not significant (FDR > 0.05) except for the ncRNA gene in the retron (*SI Appendix*, Table S1). Phage

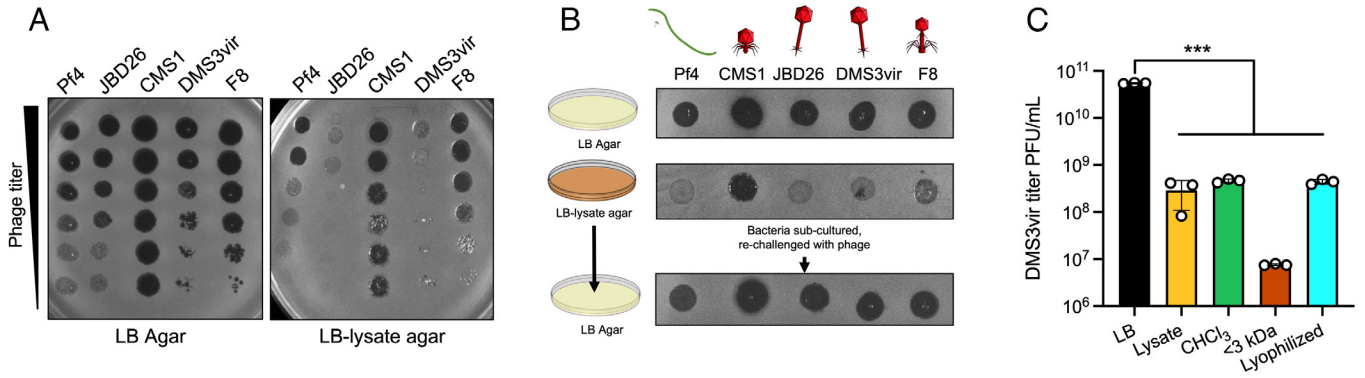


**Fig. 1.** Soluble molecules released by lysed *P. aeruginosa* cells induce a transient phage-resistant phenotype. (*A*) The indicated phage species were titered on lawns *P. aeruginosa* PAO1 growing on LB agar or LB-lysate agar after 18 h of growth. Representative images are shown. (*B*) Phages were spotted at $10^6$ plaque forming units (PFUs) in 3 µL onto lawns of *P. aeruginosa* PAO1 grown on LB agar or LB-lysate agar. Plaques were imaged after overnight (18 h) growth at 37 °C. *P. aeruginosa* growing on lysate plates were then subcultured onto LB agar plates and rechallenged with the indicated phages. Representative images are shown. (*C*) Phage DMS3vir was spotted onto lawns of *P. aeruginosa* growing on LB agar or LB agar supplemented with cell lysate, the aqueous phase of $CHCl_3$-extracted cell lysate, the aqueous phase passed through a 3 kDa membrane, or lyophilized aqueous phase extract. Results are mean ± SD of three experiments, ***$P < 0.001$.

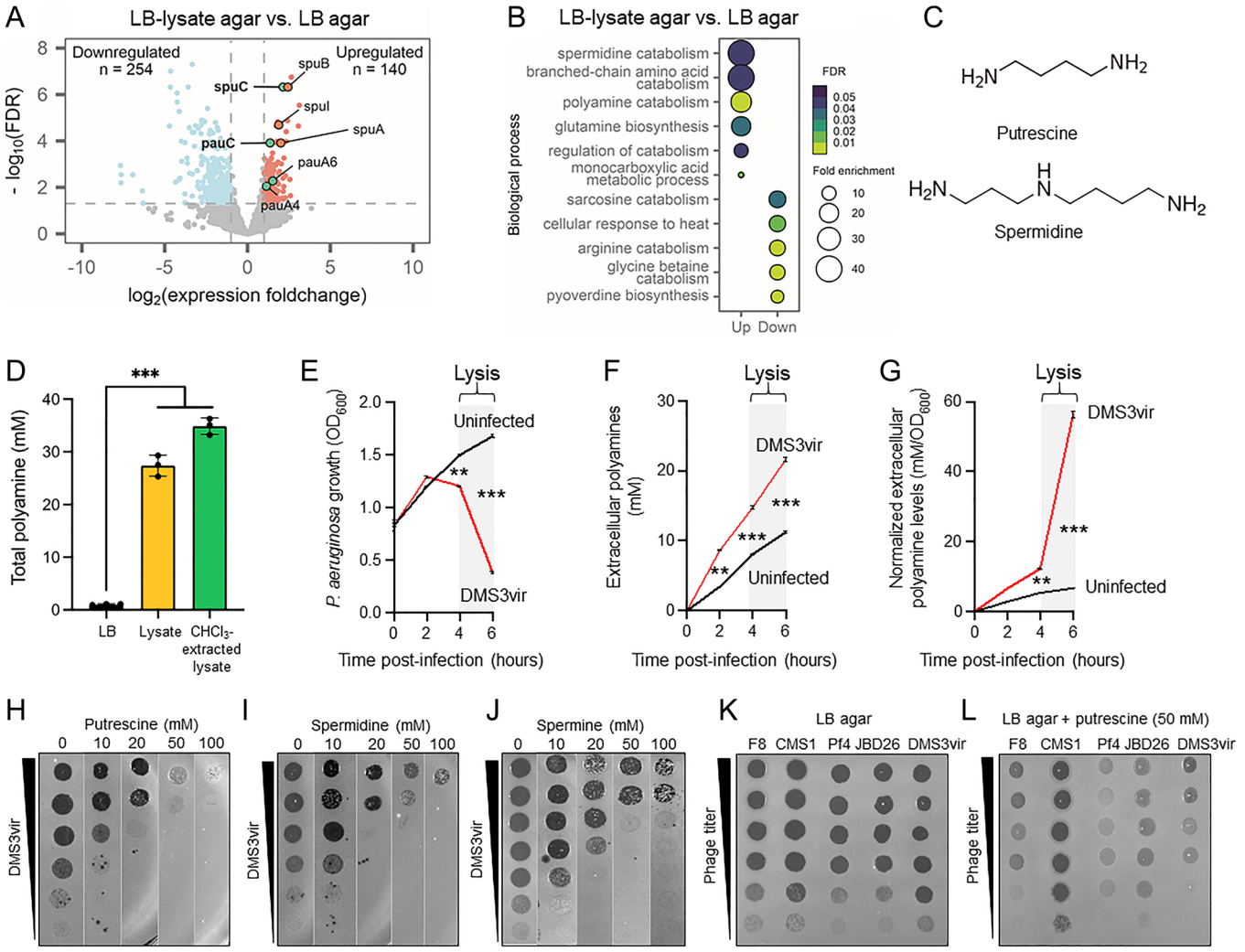


**Fig. 2.** The polyamines putrescine and spermidine induce phage resistance in *P. aeruginosa*. (*A*) Volcano plot showing differentially expressed genes in wild-type cells grown on LB-lysate agar compared with cells grown on LB agar. Red indicates up-regulated genes ($log_2$[foldchange] > 1 and false discovery rate (FDR) <0.05), and blue indicates down-regulated genes ($log_2$[foldchange] <−1 and FDR < 0.05). Nonsignificant genes are shown in gray. Polyamine metabolism and transport genes are highlighted. Data are representative of duplicate experiments. (*B*) Gene enrichment analysis of significant differentially expressed genes shown in (*A*). Dot sizes indicate fold enrichment of observed genes associated with specific Gene Ontology (GO) terms versus what is expected by random chance. (*C*) Structures of the polyamines putrescine and spermidine. (*D*) Total polyamine content in LB broth, cell lysate, and $CHCl_3$-extracted cell lysate were measured by fluorometric assay. Results are mean ± SD of three experiments, ***$P$ < 0.002. (*E*) Growth of uninfected and DMS3vir-infected (MOI 0.5) *P. aeruginosa* was monitored by Optical Density $(OD)_{600}$. Mass cell lysis is indicated by the gray box. Results are mean ± SD of three experiments, **$P$ < 0.01, ***$P$ < 0.001. (*F*) Total polyamine content was measured by fluorometric assay in culture supernatants collected from cultures shown in (*F*). Results are mean ± SD of three experiments, **$P$ < 0.01, ***$P$ < 0.001. (*G*) Polyamine concentration (mM from panel *F*) was normalized to cell density ($OD_{600}$ from panel *E*). Results are mean ± SD of three experiments, **$P$ < 0.01, ***$P$ < 0.001. (*H* and *I*) The polyamines putrescine (*I*) or spermidine (*J*) were added to LB agar at the indicated concentrations. DMS3vir was spotted onto lawns of *P. aeruginosa,* and plaques were imaged after 18 h of growth at 37 °C. (*J* and *K*) The indicated species of phage were spotted onto lawns of *P. aeruginosa* growing on LB agar or LB agar supplemented with 50 mM putrescine.

infection alone significantly induced toxin/antitoxin and Gabija genes, but not to the level that polyamines and phage infection together did (*SI Appendix*, Fig. S3 and C and Table S1). These results suggest that detection of both polyamines and phage infection is coupled to the global upregulation of phage defense systems in *P. aeruginosa*.

**Gac/Rsm Signaling Is Required for Polyamines to Induce Phage Resistance.** Our RNA-seq datasets indicate that genes associated with the Gac/Rsm pathway are significantly up-regulated by cell lysate (*SI Appendix*, Fig. S4*A*). In *P. aeruginosa,* Gac/Rsm regulates bacterial behaviors related to biofilm formation and virulence at the transcriptional level (18) (Fig. 3*A*). Gac/Rsm signaling is initiated when the sensor histidine kinase GacS is activated by unknown ligands (19). GacS phosphorylates the response regulator GacA, which induces the transcription of the small RNAs *rsmY* and *rsmZ* (20). These sRNAs bind and sequester the mRNA-binding proteins RsmA or RsmN away from their target transcripts, derepressing hundreds of mRNA species (21, 22). The sensor kinase RetS counteracts GacS activity and inactivation of the *retS* gene constitutively activates Gac/Rsm signaling (23–25).

We hypothesized that Gac/Rsm signaling regulates lysate-induced phage resistance in *P. aeruginosa*. To test this hypothesis, we used strains where the Gac/Rsm pathway was either disabled (Δ*gacS,* Δ*rsmY/Z*) or constitutively activated (Δ*retS*). Growth of these strains was not affected on LB-lysate agar plates compared with LB agar (*SI Appendix*, Fig. S4*B*). On LB agar, phage DMS3vir formed clear plaques on wild-type, Δ*gacS,* and Δ*rsmY/Z* lawns, but formed turbid plaques on Δ*retS* lawns (Fig. 3 *B*, *Top* row), suggesting that active Gac/Rsm signaling in the Δ*retS* strain is sufficient to impede DMS3vir replication. On LB-lysate agar, DMS3vir infection was suppressed on wild-type lawns and

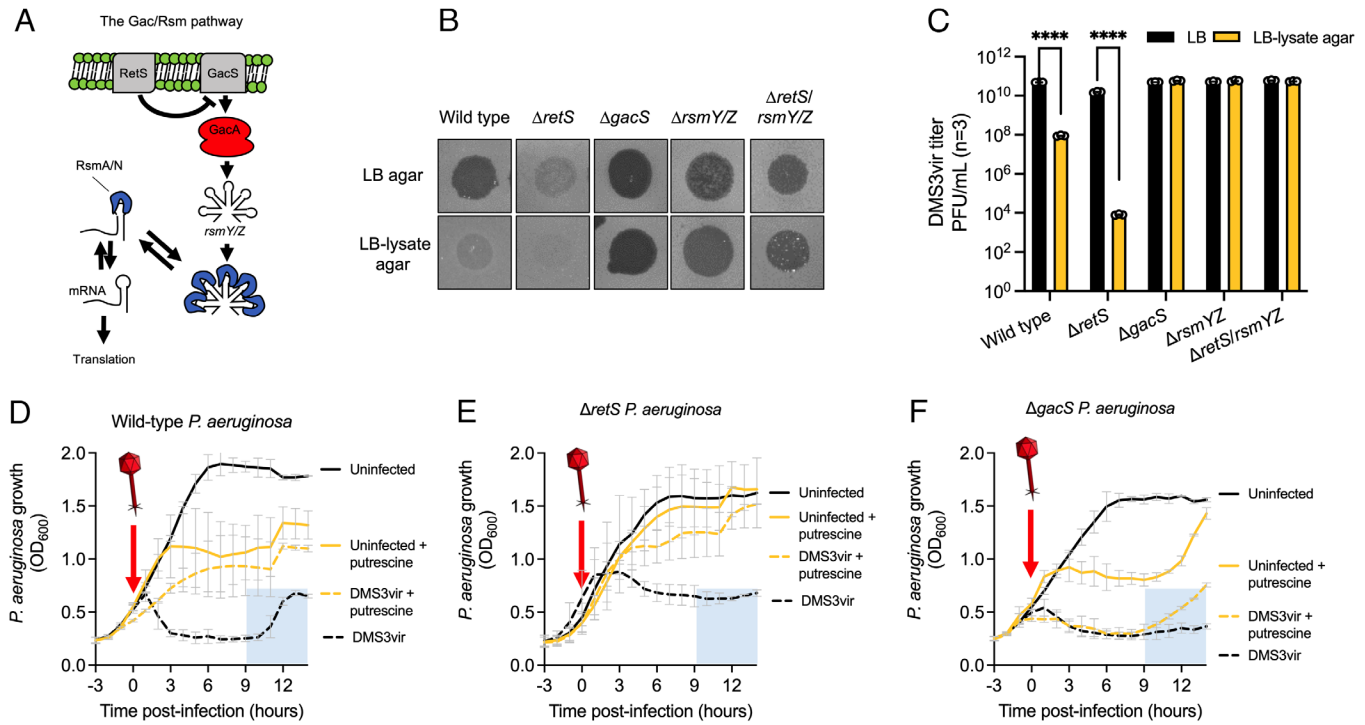


**Fig. 3.** Gac/Rsm signaling is required for polyamines to induce phage resistance. (*A*) Schematic of the Gac/Rsm pathway in *P. aeruginosa*. (*B*) Phage DMS3vir was spotted at $10^6$ PFU in 3 μL onto lawns of the indicated strains grown on LB agar or LB lysate agar. Representative plaque images are shown. (*C*) DMS3vir PFU measurements on the indicated lawns growing on LB agar or LB-lysate agar are shown. Results are mean ± SD of three experiments, ****$P < 0.0001$. (*A–C*) Growth curves of the indicated *P. aeruginosa* strains grown with (yellow) or without (black) 50 mM putrescine are shown. Cells were infected with DMS3vir at the indicated time (arrow) at a MOI of 1. Results are mean ± SD of six experiments. (*D–F*) DMS3vir titers in phage-infected cultures were measured at the indicated times. Results are mean ± SD of three experiments.

completely inhibited on Δ*retS* lawns while sensitivity to DMS3vir infection was restored in strains where Gac/Rsm signaling was disabled (Δ*gacS*, Δ*rsmY/Z*) (Fig. 3 *B* and *C*). Furthermore, deleting *rsmY* and *rsmZ* from the phage-tolerant Δ*retS* background (Δ*retS/ rsmY/Z*) restored susceptibility to phage infection on LB-lysate agar (Fig. 3 *B* and *C*).

Recent findings indicate that Gac/Rsm signaling suppresses type IV pili to prevent phage infection (26). DMS3vir uses type IV pili as a cell surface receptor (27). However, twitch assays indicate that LB-lysate agar does not affect type IV pili-dependent twitching motility of wild-type, Δ*retS*, or Δ*gacS P. aeruginosa* under the conditions tested (*SI Appendix*, Fig. S4*C*). Collectively, these results indicate that the Gac/Rsm pathway is essential for lysate-induced phage resistance.

To link polyamine-induced phage resistance to Gac/Rsm signaling, we grew wild-type, Δ*retS*, and Δ*gacS P. aeruginosa* in LB broth supplemented with 50 mM putrescine. This concentration was selected as it produces a robust phage resistance phenotype in wild-type *P. aeruginosa* for comparison to Gac/Rsm mutants. When grown with putrescine, wild-type and Δ*retS P. aeruginosa* were less susceptible to DMS3vir infection (Fig. 3 *D* and *E*, dashed lines). Compared with bacteria growing in LB, wild-type cells growing with putrescine have similar exponential growth kinetics but grow to a lower cell density (Fig. 3*D*, solid lines), suggesting a controlled exit from exponential to stationary phase growth in putrescine-exposed cells.

Disabling Gac/Rsm signaling (Δ*gacS*) restored sensitivity to DMS3vir infection (Fig. 3*F*, dashed lines). It is possible that suppressed bacterial growth by polyamines explains reduced susceptibility to phage infection. However, Δ*gacS* also displayed polyamine-induced growth suppression but remained sensitive to phage infection (Fig. 3*F*, solid lines). Note that bacterial growth on agar was not affected when plates were supplemented with 50 mM putrescine (*SI Appendix*, Fig. S4*B*). The differences in how polyamines affect bacterial growth in liquid culture versus on solid agar points to a surface-associated growth phenotype. Collectively, these observations indicate that bacterial growth suppression by polyamines is not required for polyamine-induced phage resistance.

Phage replication is inhibited when polyamines are supplied exogenously. To determine whether polyamines released from phage-infected cultures protect *P. aeruginosa* from infection, we monitored bacterial growth in cultures not supplemented with polyamines. In wild-type cultures not supplemented with polyamines, mass bacterial lysis occurs approximately 3 h postinfection, and bacterial growth resumed after approximately 9 h (Fig. 3*D*, shaded area, dashed black line). Bacteria that grew after phage infection were confirmed phage resistant (*SI Appendix*, Fig. S4*D*). This outgrowth was not observed in Δ*gacS* cultures not supplemented with polyamines (Fig. 3*F*, shaded area, dashed black line) but was observed in Δ*gacS* cultures that were supplemented with exogenous polyamines (Fig. 3*F*, shaded area, dashed yellow line). These observations are consistent with a model where polyamines and Gac/Rsm signaling protect *P. aeruginosa* from phage infection, perhaps by promoting the emergence of phage-resistant subpopulations.

**Putrescine Inhibits Phage Genome Replication.** Exogenous putrescine differentially affected DMS3vir replication in wild-type, Δ*retS*, and Δ*gacS P. aeruginosa*. In wild-type cells, putrescine reduced DMS3vir titers by ~3,500-fold compared with cells not grown with putrescine after 6 h (Fig. 4*A*). Similar observations were made in Δ*retS P. aeruginosa*, where putrescine reduced DMS3vir titers by ~1,300 fold compared with Δ*retS* cultures without

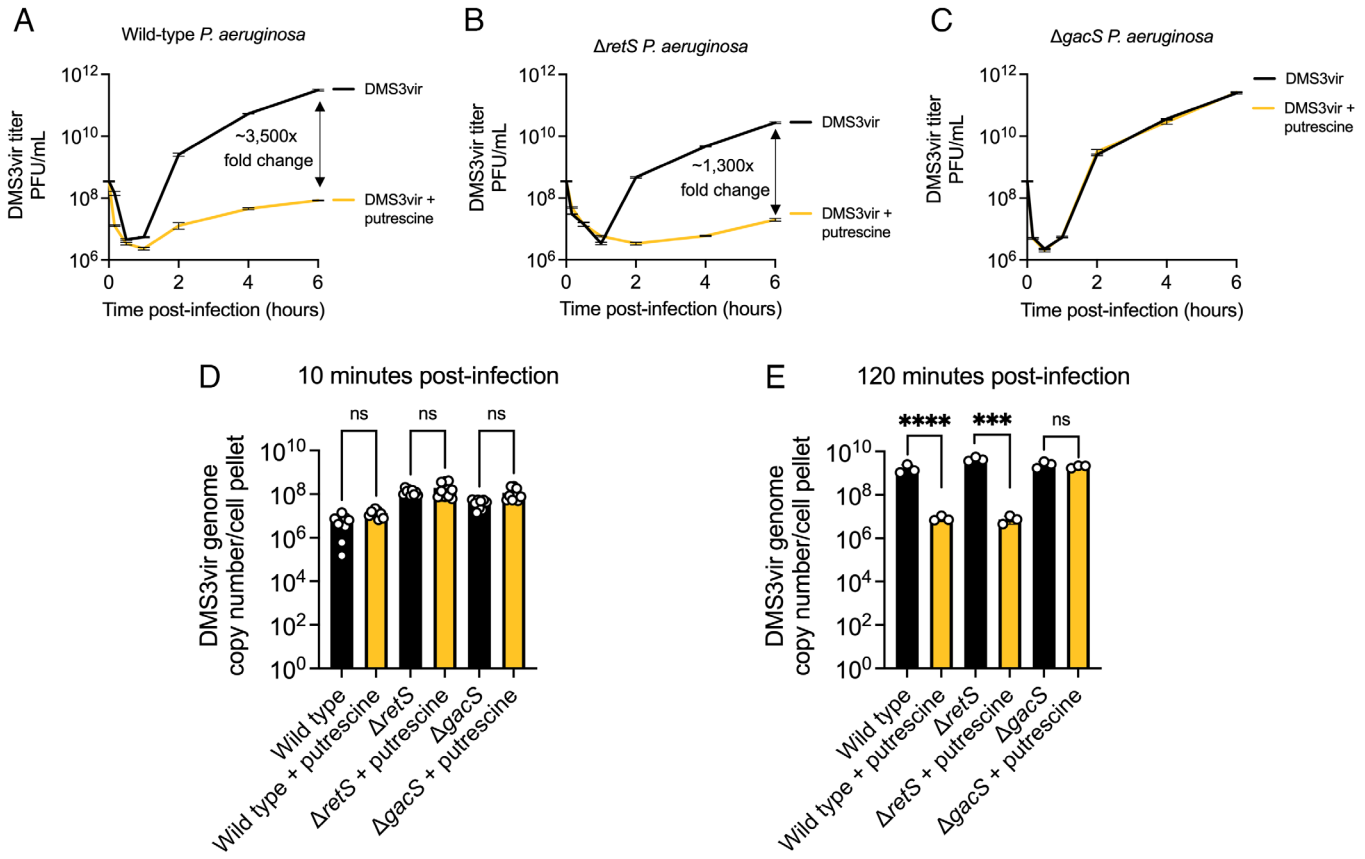


**Fig. 4.** Putrescine inhibits phage genome replication. (*A–C*) DMS3vir titers were measured in wild-type, Δ*retS*, or Δ*gacS P. aeruginosa* with (yellow) or without (black) putrescine. Results are mean ± SD of three experiments. (*D* and *E*) DMS3vir genome copy number was measured by qPCR in the indicated strains at 10 or 120 min postinfection with or without 50 mM putrescine. Absolute copy number was determined using a standard curve generated with a cloned copy of the target sequence. Results are mean ± SD of nine (*D*) or three (*E*) experiments: ****$P < 0.0001$, ***$P < 0.001$, ns (not significant).

putrescine (Fig. 4*B*). When Gac/Rsm signaling was disabled (Δ*gacS*), DMS3vir replication was not affected by putrescine and was comparable to DMS3vir replication in wild-type cells growing in LB broth (Fig. 4*C*).

To determine how polyamines affect the phage lifecycle, we measured DMS3vir genome copy numbers in cell pellets collected 10 and 120 min postinfection. At 10 min postinfection, before any progeny virions are produced (Fig. 4 *A–C*), no significant difference in DMS3vir genome copy number was observed in strains grown with or without putrescine (Fig. 4*D*). This result indicates that equivalent numbers of DMS3vir genomes were injected into cells, even when putrescine was present. These results also indicate that polyamines do not affect phage virion adsorption to bacterial cells.

After 120 min in a wild-type host grown without putrescine, DMS3vir genome copy numbers increased ~1,000-fold compared with the 10-min time point (Fig. 4*E* black bar). When putrescine was present, DMS3vir genome copy numbers remained static compared with the 10-min time point (Fig. 4*E* yellow bar). DMS3vir genome copy numbers were ~100-fold lower in Δ*retS P. aeruginosa* grown with putrescine, whereas putrescine had no effect on the DMS3vir genome copy number in Δ*gacS* bacteria grown with or without putrescine (Fig. 4*E*). These data indicate that Gac/Rsm signaling is required for putrescine to inhibit DMS3vir genome replication.

Many phage genomes exist as circular episomes at some point during their lifecycle. We hypothesized that polyamines would interfere with episomal DNA replication. To test this, we measured the copy number of pMF230, a high copy number plasmid constitutively expressing green fluorescent protein (GFP) (28). Putrescine did not affect plasmid copy number in wild-type, Δ*retS*, or Δ*gacS P. aeruginosa* (*SI Appendix*, Fig. S5*A*). Furthermore, transcription of *gfp* from pMF230 (as measured by qRT-PCR) was not significantly affected by putrescine in any strain or condition tested (*SI Appendix*, Fig. S5*B*). These results indicate that episomal DNA replication and transcription are not affected by polyamines, raising the possibility that polyamines specifically inhibit phage DNA replication.

**DMS3vir Induces Gac/Rsm-Dependent Intracellular Polyamine Accumulation.** To gain insight into how polyamines and phage infection affect the *P. aeruginosa* host, we performed RNA-seq on wild-type cells grown with or without putrescine for 3 h followed by infection with DMS3vir at an multiplicity of infection (MOI) of 1.

Two hours postinfection, DMS3vir transcription was strongly down-regulated in cells grown in putrescine compared with cells grown without putrescine (Fig. 5*A*, large blue dot). In DMS3vir-infected cells grown with 50 mM putrescine, we were surprised to find that polyamine catabolism genes are significantly down-regulated compared with uninfected cells grown with putrescine (Fig. 5*B*).

We hypothesized that downregulation of polyamine catabolism genes in phage-infected cells would cause intracellular polyamine levels to increase. To test this, cell pellets were harvested, washed, lysed with $CHCl_3$, and total polyamines measured using a fluorometric assay. Polyamine concentrations were then normalized to bacterial density ($OD_{600}$).

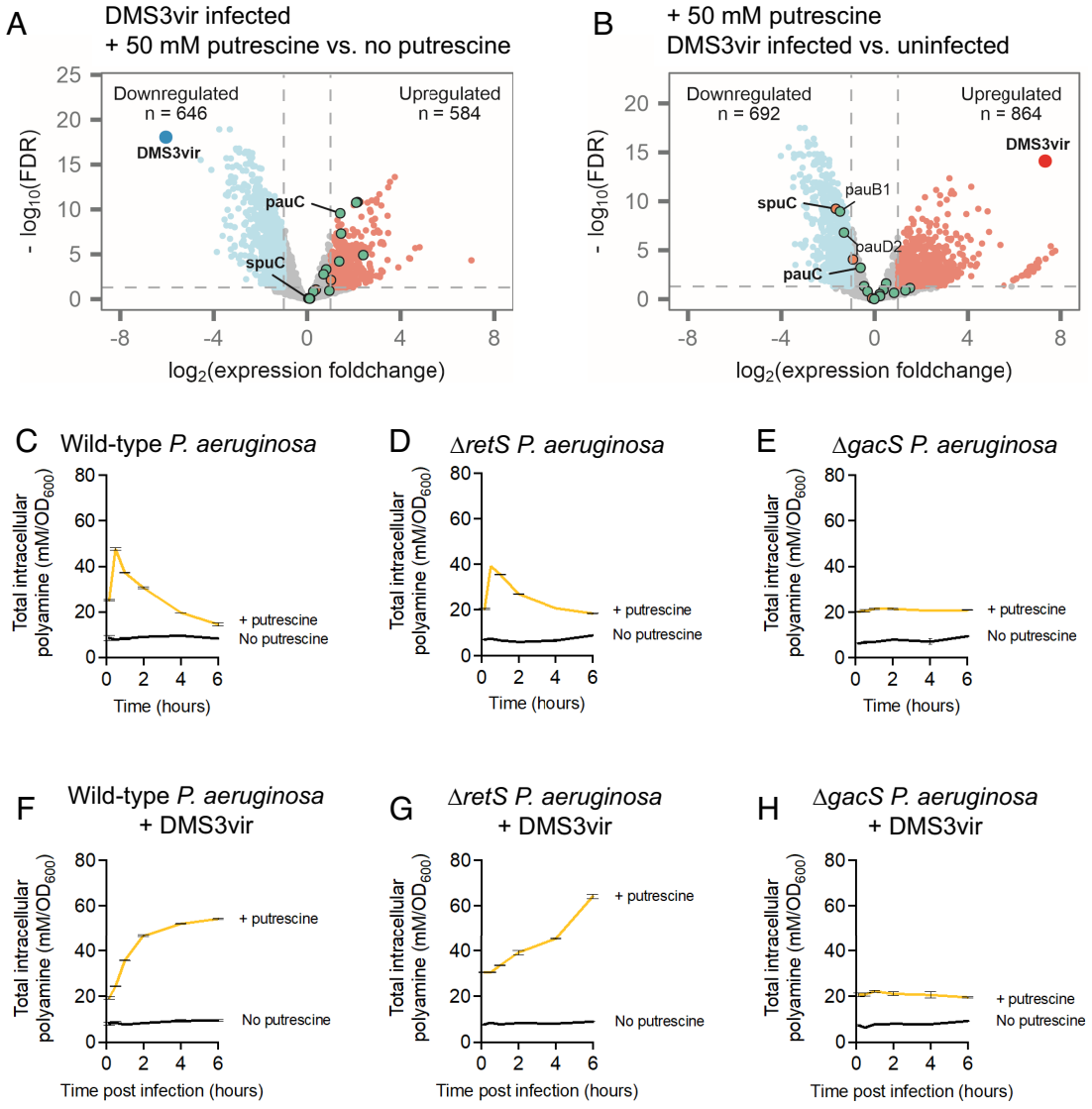


**Fig. 5.** DMS3vir infection down-regulates polyamine catabolism genes and induces Gac/Rsm-dependent intracellular polyamine accumulation. Volcano plots showing differentially expressed genes in (*A*) DMS3vir-infected cells cultured with or without 50 mM putrescine or (*B*) DMS3vir-infected versus uninfected cells grown with 50 mM putrescine. Red dots indicate up-regulated genes ($\log_2$[foldchange] > 1 and FDR < 0.05), and blue dots indicate down-regulated genes ($\log_2$[fold change] < −1 and FDR < 0.05). Nonsignificant genes are shown in gray. Genes involved in polyamine and putrescine catabolism are highlighted. Reads that mapped to the DMS3vir genome are indicated by large blue or red dots in panels *A* or *B*, respectively. (*C*–*H*) The indicated strains were grown with (yellow) or without (black) 50 mM putrescine in LB broth for the indicated times at 37 °C. Bacterial density ($OD_{600}$) and total intracellular polyamine were measured and normalized intracellular polyamine levels in (*C*–*E*) uninfected or (*F*–*H*) DMS3vir-infected cultures. Results are mean ± SD of duplicate experiments.

In uninfected wild-type, Δ*retS*, and Δ*gacS* cells growing in LB, basal intracellular polyamine levels were all approximately 8 mM/$OD_{600}$ (Fig. 5 *C*–*E*, black lines). In wild-type and Δ*retS P. aeruginosa* grown with putrescine, intracellular polyamine levels spiked to over 40 mM/$OD_{600}$ during the first 30 min and returned to near basal levels over the course of 6 h (Fig. 5 *C* and *D*, yellow lines). Intracellular polyamine levels in the Δ*gacS* mutant did not fluctuate and remained at 20 mM/$OD_{600}$ over the course of the experiment (Fig. 5*E*, yellow line). These results indicate a role for Gac/Rsm signaling in regulating intracellular polyamine homeostasis in *P. aeruginosa*.

In *P. aeruginosa* growing in LB, DMS3vir infection did not affect intracellular polyamine levels in wild type, Δ*retS*, or Δ*gacS*; all remained at ~8 mM/$OD_{600}$ (Fig. 5 *F*–*H*, black lines). In the presence of putrescine, however, DMS3vir infection caused intracellular polyamine levels to increase to and remain at ~50 mM/$OD_{600}$ over the course of the entire experiment in both wild-type and Δ*retS P. aeruginosa* (Fig. 5 *F* and *G*, yellow lines). When Δ*gacS* cells growing in putrescine were infected by DMS3vir, intracellular polyamine levels remained unchanged at ~20 mM/$OD_{600}$ (Fig. 5*H*, yellow line), comparable to uninfected Δ*gacS* cells grown with putrescine (Fig. 5*E*, yellow line). This observation may explain why the Δ*gacS* strain has a polyamine-induced growth defect but is still sensitive to phage infection (Fig. 3*F*); intracellular polyamine levels may be sufficiently high to affect bacterial growth, but not high enough to significantly inhibit phage replication.

We also measured extracellular polyamine concentrations over 6 h in wild-type cells grown with 50 mM putrescine +/− DMS3vir infection. Over 6 h, extracellular polyamine concentrations fell faster in phage-infected cells (50 mM to ~15 mM) compared with uninfected cells (50 mM to ~25 mM) (*SI Appendix*, Fig. S6), suggesting that phage-infected cells actively take up extracellular polyamines.

Collectively, these results indicate that in response to phage infection, polyamine catabolism is down-regulated causing intracellular polyamine levels to increase, so long as Gac/Rsm signaling is intact.

**Phage Replication Is Not Required to Induce Intracellular Polyamine Accumulation.** We next tested whether phage replication was required to induce polyamine accumulation in *P. aeruginosa*. To do so, we inactivated phage DMS3vir by irradiating with ultraviolet (UV) light (*SI Appendix*, Fig. S7*A*). *P. aeruginosa* cells growing in putrescine were then infected with untreated DMS3vir or UV-irradiated DMS3vir and intracellular polyamine levels were measured over time. Both untreated and UV-irradiated phages induced intracellular polyamine accumulation (*SI Appendix*, Fig. S7*B*), indicating that phage replication is not required to trigger intracellular polyamine accumulation.

**Linear DNA Induces Intracellular Polyamine Accumulation.** Polyamines protect *P. aeruginosa* from diverse phage species, suggesting a common phage-associated signal induces polyamine accumulation. A common feature of many phages is that they either inject linear DNA into the host cell or produce linear DNA at some point during their natural replication cycle (e.g., rolling circle replication) (29). To test the hypothesis that linear DNA induces intracellular polyamine accumulation, we expressed the homing endonuclease I-SceI (pI-SceI) in cells transformed with a high copy number plasmid encoding the I-SceI cut site (pCut) (Fig. 6*A*) or a plasmid not encoding the I-SceI cut site (pEmpty) as a negative control. PCR was used to confirm the presence of pI-SceI nuclease (Fig. 6*B*) and the presence of linear pCut plasmid DNA in vivo (Fig. 6*C*). We then measured growth (Fig. 6*D*) and intracellular polyamine levels (Fig. 6 *E* and *F*) in *P. aeruginosa* carrying linearized or circular plasmid DNA.

Linearized pCut plasmid DNA induced significant ($P < 0.01$) intracellular polyamine accumulation compared with cells carrying the circular pEmpty plasmid (Fig. 6*F*), indicating that linear DNA is sufficient to induce intracellular polyamine accumulation in *P. aeruginosa*.

**The N4-Like Phage CMS1 Does Not Induce Intracellular Polyamine Accumulation.** Cell lysate and putrescine inhibited phages F8, DMS3vir, JBD26, and Pf4, but not phage CMS1 (Figs. 1*A* and 3 *F* and *G*). One possible explanation is that phage CMS1 does not induce polyamine accumulation. To test this, we measured intracellular polyamine levels in wild-type, Δ*retS*, and Δ*gacS* bacteria over time. CMS1 infection did not induce intracellular polyamine accumulation in wild-type or Δ*retS* cells (*SI Appendix*, Fig. S8 *A* and *B*), and intracellular polyamine levels in the Δ*gacS* strain remained low near basal levels (*SI Appendix*, Fig. S8*C*). Putrescine did not affect CMS1 titers in any strain or condition (*SI Appendix*, Fig. S8 *D*–*F*).

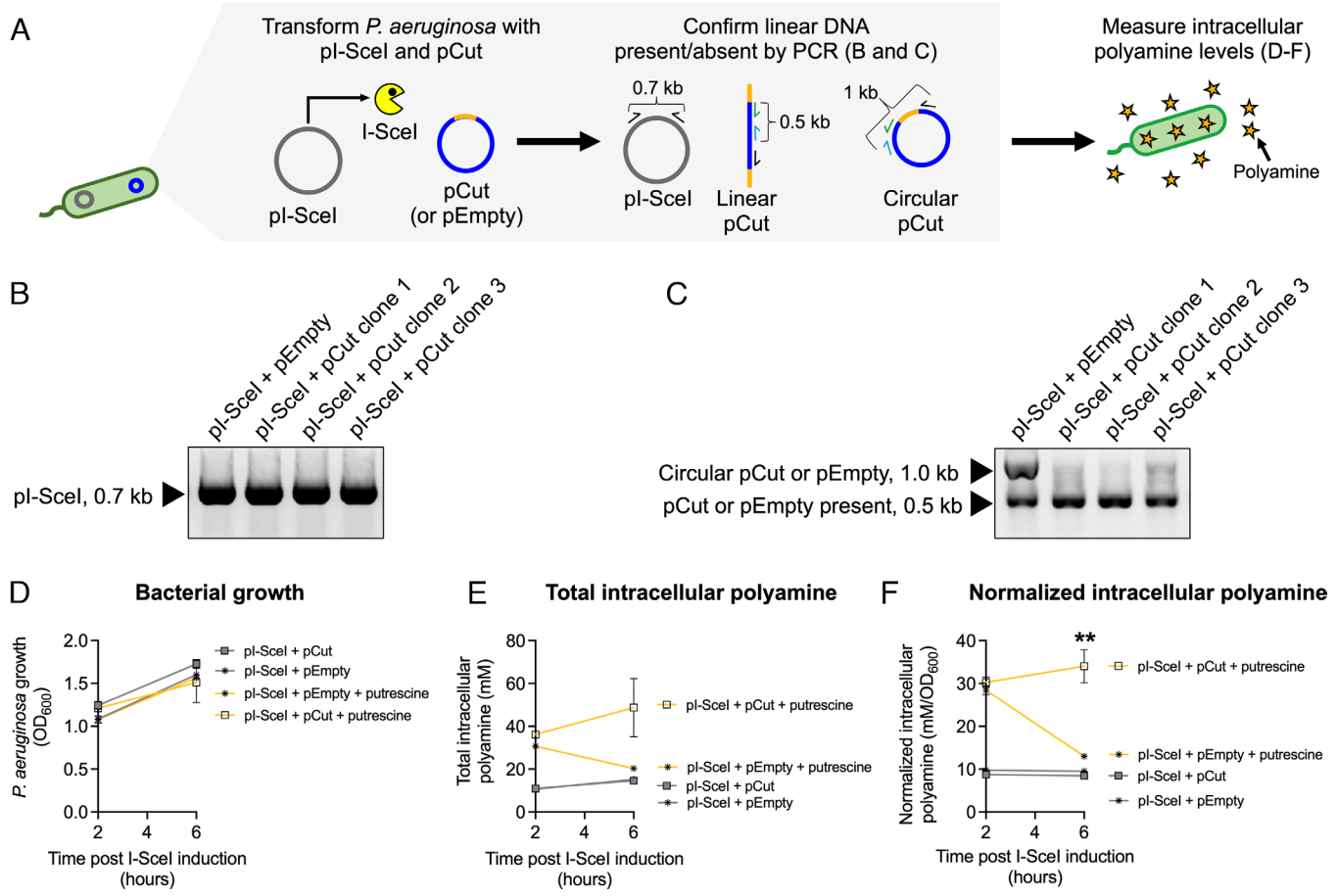


**Fig. 6.** Linear DNA induces intracellular polyamine accumulation. (*A*) Experimental design. pI-SceI encodes the inducible homing endonuclease I-SceI. pCut encodes the 18-bp I-SceI cut site (orange), and the empty vector control pEmpty lacks the cut site. (*B*) The presence of plasmid pI-SceI was confirmed by PCR in *P. aeruginosa* PAO1 transformants 6 h post I-SceI induction. (*C*) The presence or absence of linear pCut or pEmpty plasmid DNA was confirmed by PCR in transformants 6 h post I-SceI induction. (*D*–*F*) Transformants were grown with (yellow) or without (gray) 50 mM putrescine in LB broth for the indicated times at 37 °C. (*D*) Bacterial density ($OD_{600}$) and (*E*) total intracellular polyamine were measured. (*F*) Intracellular polyamine levels were normalized to bacterial density ($OD_{600}$). Results are mean ± SD of triplicate experiments, $^{**}P < 0.01$ compared with pI-SceI + pEmpty + putrescine.

These results indicate that CMS1 infection prevents Gac/Rsm-dependent polyamine accumulation.

CMS1 is an N4-like lytic phage (30) and we wondered if other N4-like phages also escape inhibition by polyamines. To test this idea, we performed phage challenge experiments with KPP21 (31), another N4-like phage, which we find also escapes inhibition by polyamines (*SI Appendix*, Fig. S9). These results suggest that some phages have evolved mechanisms to control host intracellular polyamine levels, which is consistent with a role for polyamines in phage defense.

## Discussion

A role for polyamines in phage replication was initially uncovered during the experiment by Hershey and Chase demonstrating that T2 phage inject only their DNA into host cells, verifying that DNA (and not protein) carries genetic information (32). The phage preparations used in those classic experiments contained an unknown "minor phage component" referred to as Substance A (33), which was later identified as polyamines (34). Polyamines bind to and neutralize negatively charged DNA. In some phage species, this is thought to facilitate phage genome condensation and packaging into procapsids (35, 36). However, in other phage species, polyamines inhibit phage replication (37, 38).

The present study expands our understanding of how polyamines affect phage replication in the opportunistic pathogen *P. aeruginosa* (*SI Appendix*, Fig. S10). Our results suggest that Gac/Rsm-dependent intracellular polyamine accumulation inhibits phage genome replication and transcription. One possible mechanism for how polyamines may inhibit phage replication in *P. aeruginosa* involves the direct condensation or aggregation of phage DNA by high levels of intracellular polyamines, which is known to make template DNA unavailable for transcription by RNA polymerase (39) or replication by DNA polymerase (40). Polyamines affect other enzymes involved in DNA replication as well. For example, Mu-like phages like DMS3vir copy their DNA by replicative transposition, which requires DNA gyrase (41). Depending on the bacterial species, polyamines can either inhibit or enhance DNA gyrase activity (13). Thus, it is possible that intracellular polyamine accumulation could inhibit DMS3vir replication by affecting DNA gyrase activity in *P. aeruginosa*.

Our results indicate a critical role for Gac/Rsm signaling in regulating intracellular polyamine levels in *P. aeruginosa*. The Gac/Rsm pathway contains two major RNA-binding proteins, RsmA and RsmN (Fig. 3*A*) (22, 42). The RsmA regulon includes genes encoding two periplasmic polyamine-binding proteins (PA2711 and PA0295) and the acetylpolyamine aminohydrolase PA1409 (42). Polyamine catabolism genes are also in the RsmN regulon; the 5′-CANGGAYG motif recognized by RsmN is present in the polyamine metabolism genes *spuA, speC, pauB3, pauA5,* and *pauC* (22).

Intracellular polyamine accumulation was triggered by DMS3vir phage infection and linear DNA, which is analogous to how some phage defense systems detect phage infection. For example, the DrmAB complex of defence island system associated with restriction–modification (DISARM) systems binds to linear DNA substrates with a 5′-overhang, allowing this defense system to detect infection by a wide range of phage species (29). How linear DNA induces intracellular polyamine accumulation is not known but may involve DNA-binding protein(s) analogous to DrmAB that discriminate DNA targets based on structure as opposed to sequence.

Our results indicate that elevated intracellular polyamine levels and phage infection transcriptionally up-regulate phage defense systems. Consistent with our observations, polyamines are known to modulate the activity of several restriction endonucleases (43, 44) and that polyamines strongly increase the fidelity of the *Escherichia coli* CRISPR Cas1-Cas2 integrase, which has the effect of decreasing off-target spacer acquisition (45). Acquisition of immunity against certain phages may also affect polyamine accumulation in *P. aeruginosa*. For example, a recent study compared the transcriptomes of uninfected and DMS3vir-infected *P. aeruginosa* (46). The *P. aeruginosa* strain used in that study encodes two CRISPR spacers that target DMS3vir, giving cells preexisting immunity to infection (47). In DMS3vir-immune strains, DMS3vir infection caused polyamine catabolism genes to be significantly up-regulated, which contrasts with our observations where DMS3vir infection down-regulated polyamine catabolism genes. While there are many possible explanations (e.g., the presence versus absence of exogenous putrescine), it is possible that polyamine catabolism is differentially regulated in immune versus naïve hosts that do not have preexisting immunity against DMS3vir.

We observed the strongest phage resistance phenotypes in cultures supplemented with exogenous putrescine. We hypothesize that exogenous polyamine concentrations in phage-infected cultures do not reach sufficiently high levels to inhibit phage replication until after the majority of bacteria have been lysed. The release of polyamines by dead kin cells may increase the chance that a subpopulation of cells survive infection, which is consistent with the observed outgrowth in wild-type cultures infected by DMS3vir.

Intracellular polyamine accumulation inhibited the replication of most but not all phages tested. The N4-like phages evaded inhibition by polyamines by preventing intracellular polyamine accumulation. Previous work demonstrates that multiple N4-like phage species encode proteins that bind to enzymes related to *P. aeruginosa* polyamine metabolism in bacterial two-hybrid assays (48, 49). Collectively, these observations suggest that N4-like phages modulate host polyamine metabolism to escape inhibition by intracellular polyamine accumulation.

The ability to detect danger signals is a fundamental feature of innate immune systems. Our data support a model where *P. aeruginosa* senses polyamines and linear DNA as danger signals to make threat assessments of cellular injury. Future studies determining the precise mechanisms by which linear DNA is detected, how Gac/Rsm signaling regulates intracellular polyamine levels, and whether other molecules serve as bacterial danger signals will provide valuable insights into bacterial immune systems. Our results also highlight danger sensing as a shared behavior across biological kingdoms, which may reveal generalizable principles of cellular responses to viral infection and cellular injury.

## Methods

**Bacterial and Phage Strains, Growth Conditions, Plasmids, and Primers.** Bacterial strains, phages, plasmids, and their sources are listed in Table 1. Deletion mutants were constructed using allelic exchange and Gateway technology, as described previously (50). Primer sequences are listed in Table 2. Unless indicated otherwise, bacteria were grown in LB at 37 °C with shaking and supplemented with antibiotics (Sigma) or 0.1% arabinose when appropriate. Unless otherwise noted, antibiotics were used at the following concentrations: gentamicin (10 or 30 μg $mL^{-1}$), ampicillin (100 μg $mL^{-1}$), and carbenicillin (300 μg $mL^{-1}$).

**Cell Lysate and Polyamine Agar Plate Preparation.** *P. aeruginosa* PAO1 cells were pelleted, washed in phosphate buffered saline (PBS), and resuspended in fresh lysogeny broth (LB). Bacteria were then lysed by infecting with DMS3vir (MOI 1) or sonication. Cell debris was removed by centrifugation and any virions removed by filtering through a 100 kDa molecular weight cutoff (MWCO) membrane. Agar plates were prepared by adding agar powder (1.5% w/vol) to the

**Table 1. Bacterial strains, phage, and plasmids used in this study**

| Strain | Description | Source |
|---|---|---|
| *E. coli* | | |
| DH5α | Plasmid maintenance/propagation | New England Biolabs |
| S17 | λpir-positive strain used for conjugation | New England Biolabs |
| *P. aeruginosa* | | |
| PAO1 | Wild type | (51) |
| PAO1 Δ*retS* | Clean deletion of *retS* from PAO1 | (25) |
| PAO1 Δ*gacS* | Clean deletion of *gacS* from PAO1 | (52) |
| PAO1 Δ*rsmY/Z* | Clean deletion of *rsmY* and *rsmZ* from PAO1 | This study |
| PAO1 Δ*retS/rsmY/Z* | Clean deletion of *rsmY* and *rsmZ* from PAO1 Δ*retS* | This study |
| Bacteriophage | | |
| Pf4 | Inoviridae | (53) |
| JBD26 | Siphoviridae | (54) |
| CMS1 | Podoviridae | (51) |
| DMS3vir | Siphoviridae | (10) |
| F8 | Myoviridae | (55) |
| Plasmids | | |
| pI-SceI | I-SceI nuclease cloned into pHERD30T | This study |
| pCut | I-SceI cut site cloned into pUCP18 | This study |
| pEmpty | pUCP18 | (56) |
| pEX18Gm | Allelic exchange suicide vector | (57) |

bacterial lysate. Polyamines [Putrescine dihydrochloride (MP Biomedicals) and spermidine trihydrochloride (Sigma)] were added to sterile molten LB agar (1.5%) at the indicated final concentrations. Molten agar was mixed until polyamine powder was fully dissolved and then poured to make polyamine-supplemented agar plates.

**Plaque Assays.** Plaque assays were performed using lawns of the indicated strains grown on the indicated plates. Phages in filtered supernatants were serially diluted 10× in PBS and spotted onto lawns of the indicated strain. Plaques were imaged after 18 h of growth at 37 °C.

**Growth Curves.** Overnight cultures were diluted to an $OD_{600}$ of 0.05 in 96-well plates containing LB and, if necessary, the appropriate antibiotics, cell lysate, or polyamines. After 3 h of growth, strains were infected with the indicated phage and growth measurements resumed. $OD_{600}$ was measured using a CLARIOstar (BMG Labtech) plate reader at 37 °C with shaking prior to each measurement.

**qPCR Measurement of DMS3vir Genome Copy Number.** Whole genomic DNA was extracted from PAO1 pellets that had been frozen at −80 °C. DNA was purified using the Monarch Genomic DNA kit per the manufacturer's protocol.

**Table 2. Primers used in this study**

| Name | Sequence 5′ - 3′ |
|---|---|
| Δ*rsmY*-out F | CGGCGAGCGGAACTATTACA |
| Δ*rsmY*-out R | AGGCGGAACTGAACCACATG |
| Δ*rsmZ*-out F | CCAGGCGATTTTCTCCGAAGA |
| Δ*rsmZ*-out R | GCCAAAAACGCTCGGTGAAT |
| DMS3 qPCR F | TCGACTCGGAACAGCAGAAC |
| DMS3 qPCR R | TAGAACATCCACTGCGCCAG |
| pI-SceI F | GCGGAATTCatgcatatgaaaaac |
| pI-SceI R | GCGTCTAGAttatttcaggaaagtt |
| pCut F | AACAGCGGATCGTTCTGG |
| pCut R | CAACTTGAAGTCCTTGATCG |
| M13 R | CAGGAAACAGCTATGAC |

Primers for qPCR were created for DMS3vir-26, a hypothetical protein (DMS3 qPCR F and R, Table 2). All samples, standards, and controls were run in triplicate in 10 μL reactions using SYBR SsoAdvanced Universal Green Supermix, 1 ng genomic DNA/reaction, and gene-specific primers (300 nM final concentration). Samples were run on a CFX Connect Real-Time System (Bio-Rad) using cycle conditions: 98 °C for 1 min followed by 45 cycles of 98 °C for 15 s and 60 °C for 30 s, followed by a melt curve from 65 °C to 98 °C by 0.5 °C steps. Data were captured with CFX Maestro and were organized in Excel and analyzed and visualized in Prism 9. A standard curve with a linear regression trendline was created and the log copy number for each condition was calculated. A one-way ANOVA with Tukey's multiple comparison test was performed in Prism on log-transformed data to compare the mean copy number at each time point with those of each condition and strain.

**Polyamine Measurements.** Polyamines were measured using the Total Polyamine Assay Kit (MAK349, Sigma). A 100 μL aliquot of the indicated bacterial cultures was collected, centrifuged, washed with 1× PBS, and resuspended in PBS. Bacteria were lysed with 1:10 vol/vol chloroform, vortexed, and incubated at room temperature for 2 h. The solution was centrifuged, and the top aqueous layer was collected. Following the manufacturer's instructions, 1.0 μL of the collected sample was mixed with the Total Polyamine Assay Kit reagents, incubated at 37 °C for 30 min, and read using a CLARIOStar plate reader using end point fluorescence ($\lambda_{ex}$ = 535 nm/$\lambda_{em}$ = 587 nm). Polyamine concentrations were determined by comparing values to a standard curve constructed from known concentrations of putrescine. Values were then normalized to $OD_{600}$ measurements taken from the original bacterial cultures.

**RNA Purification and RNA-seq.** Total RNA was extracted from the indicated strains and conditions 2 h post phage infection using TRIzol. The integrity of the total cellular RNA was evaluated using RNA tape of Agilent TapeStation 2200 before library preparation. All RNA samples were of high integrity with a RIN score of 7.0 or more. rRNA was first depleted from 500 ng of each sample using MICROBExpress Kit (AM1905, Fisher) following the manufacture's instruction. The rRNA-depleted total RNA was subjected to library preparation using NEBNext® Ultra™ II RNA Library Prep Kit (E7700, New England Biolabs) and barcoded with NEBNext Multiplex Oligos for Illumina (E7730, New England Biolabs) following the manufacturer's instructions. The libraries were pooled with equal amounts of moles, further sequenced using MiSeq Reagent V3 (MS-102-3003, Illumina) for

pair-ended, 600-bp reads, and demultiplexed using the build-in bcl2fastq code in Illumina sequence analysis pipeline. Raw sequencing reads have been deposited as part of BioProject PRJNA806967 in the NCBI SRA database.

**RNA-seq Data Analysis.** Quality control analyses of RNA-seq datasets included clustered correlation matrix of gene expression levels and multidimensional scaling analyses (*SI Appendix*, Fig. S11). One of the replicates (LB, replicate 4) was identified as an outlier and removed from the further analyses. RNA-seq reads were aligned to the reference *P. aeruginosa* PAO1 genome (GenBank: GCA_000006765.1), mapped to genomic features, and counted using Rsubread package v1.28.1 (58). In viral challenge assays, the DMS3 phage genome (GenBank: DQ631426.1) was concatenated with PAO1 genome and treated as a single genomic feature. Count tables produced with Rsubread were normalized and tested for differential expression using edgeR v3.34.1 (59) (Dataset S1). Genes with ≥twofold expression change and a false discovery rate (FDR) below 0.05 were considered significantly differential. Functional classification and Gene Ontology (GO) enrichment analysis were performed using PANTHER classification system (http://www.pantherdb.org/) (60). RNA-seq analysis results were plotted with ggplot2 and pheatmap packages in R.

**Linearized Plasmid DNA Assay.** pI-SceI was constructed by cloning the I-sceI nuclease from pSLTS [a gift from Shelley Copley, Addgene plasmid #59386, (61)] cloned into the expression vector pHERD30T between the EcoRI and XbaI sites using primers I-SceI F and I-SceI R (Table 2). Restriction cloning sites in primer sequences are indicated by capital letters. pCut was constructed by cloning the I-SceI recognition sequence (TAGGGATAACAGGGTAAT) into pUCP18 between the HindIII and EcoRI sites. pEmpty is simply the empty pUCP18 vector. Primers used to screen for the presence/absence of circular and linear plasmid DNA are as follows: pCutF and M13R produce a 1-kb product indicating the presence of circular pCut (these primers will not amplify linearized pCut DNA). pCutF and pCutR produce a 0.5-kb product indicating the presence of both linear and circular forms of pCut. Clones carrying pI-SceI and confirmed linearized pCut plasmid DNA or those carrying pEmpty were grown with or without 50 mM putrescine in LB broth for the indicated times. Intracellular polyamines were measured as described above.

**DMS3vir UV Irradiation.** First, 250 µL 5 × $10^5$ PFU/mL DMS3*vir* in SM buffer was added to a 48-well polystyrene plate (Falcon #351178). The phages were then UV irradiated using a Stratalinker 1800 UV cross-linker (UV 254 nm at 120,000 µW/$cm^2$) for 3 h. Phage titers were determined by plaque assays on lawns of PAO1. Finally, the UV-irradiated phages were used to infect *P. aeruginosa* (MOI = 1), followed by growth curve and total intracellular polyamine analyses.

**Statistical Analyses.** Unless specified otherwise, differences between datasets were evaluated by Student's *t* test, using GraphPad Prism version 5.0 (GraphPad Software). *P* values of <0.05 were considered statistically significant.

**Data, Materials, and Software Availability.** RNAseq FASTQ data have been deposited in NCBI SRA (PRJNA806967) (11).

**ACKNOWLEDGMENTS.** P.R.S. was supported by NIH grants R01AI138981 and P30GM140963. B.W. was supported by NIH grant R35GM134867. P.E. was supported by NIH grant R35GM133617. A.A.N. was supported by NIH grant 1K99AI171893. This article was prepared while DeAnna Bublitz was employed at the University of Montana prior to the NIH. The opinions expressed in this article are the authors' own and do not reflect the view of the NIH, the Department of Health and Human Services, or the US government.

Author affiliations: [a]Division of Biological Sciences, University of Montana, Missoula, MT 59812; [b]Department of Microbiology and Cell Biology, Montana State University, Bozeman, MT 59717; [c]Department of Cell Biology, Microbiology and Molecular Biology, University of South Florida, Tampa, FL 33620; and [d]Department of Bacteriology, Graduate School of Medicine Dentistry and Pharmaceutical Sciences, Okayama University, Okayama 700-8558, Japan

1. P. Matzinger, The danger model: A renewed sense of self. *Science* **296**, 301–305 (2002).
2. D. Zhivaki, J. C. Kagan, Innate immune detection of lipid oxidation as a threat assessment strategy. *Nat. Rev. Immunol.* **22**, 322–330 (2021), 10.1038/s41577-021-00618-8.
3. H. Kono, K. L. Rock, How dying cells alert the immune system to danger. *Nat. Rev. Immunol.* **8**, 279–289 (2008).
4. A. A. Gust, R. Pruitt, T. Nurnberger, Sensing danger: Key to activating plant immunity. *Trends Plant Sci.* **22**, 779–791 (2017).
5. C. A. Janeway Jr., Approaching the asymptote? Evolution and revolution in immunology. *Cold Spring Harb. Symp. Quant. Biol.* **54**, 1–13 (1989).
6. M. LeRoux, S. B. Peterson, J. D. Mougous, Bacterial danger sensing. *J. Mol. Biol.* **427**, 3744–3753 (2015).
7. M. LeRoux *et al.*, Kin cell lysis is a danger signal that activates antibacterial pathways of Pseudomonas aeruginosa. *Elife* **4**, e05701 (2015).
8. S. Bhattacharyya, D. M. Walker, R. M. Harshey, Dead cells release a "necrosignal" that activates antibiotic survival pathways in bacterial swarms. *Nat. Commun.* **11**, 4157 (2020).
9. E. Tzipilevich, O. Pollak-Fiyaksel, B. Shraiteh, S. Ben-Yehuda, Bacteria elicit a phage tolerance response subsequent to infection of their neighbors. *Embo J.* **41**, e109247 (2021), 10.15252/embj.2021109247.
10. K. C. Cady, J. Bondy-Denomy, G. E. Heussler, A. R. Davidson, G. A. O'Toole, The CRISPR/Cas adaptive immune system of Pseudomonas aeruginosa mediates resistance to naturally occurring and engineered phages. *J. Bacteriol.* **194**, 5728–5738 (2012).
11. C. de Mattos, P. Secor, Pseudomonas aeruginosa infected by phage DMS3vir with or without cell lysate or polyamines. *Sequence Read Archive (SRA).* https://www.ncbi.nlm.nih.gov/bioproject/PRJNA806967. Deposited 14 February 2022.
12. R. Banerji, P. Kanojiya, A. Patil, S. D. Saroj, Polyamines in the virulence of bacterial pathogens of respiratory tract. *Mol. Oral. Microbiol.* **36**, 1–11 (2021).
13. A. Duprey, E. A. Groisman, DNA supercoiling differences in bacteria result from disparate DNA gyrase activation by polyamines. *PLoS Genet.* **16**, e1009085 (2020).
14. P. Shah, E. Swiatlo, A multifaceted role for polyamines in bacterial pathogens. *Mol. Microbiol.* **68**, 4–16 (2008).
15. A. Herrero Del Valle *et al.*, Ornithine capture by a translating ribosome controls bacterial polyamine synthesis. *Nat. Microbiol.* **5**, 554–561 (2020).
16. F. Tesson *et al.*, Systematic and quantitative view of the antiviral arsenal of prokaryotes. *Nat. Commun.* **13**, 2561 (2022).
17. L. J. Payne *et al.*, Identification and classification of antiviral defence systems in bacteria and archaea with PADLOC reveals new system types. *Nucleic Acids Res.* **49**, 10868–10878 (2021).
18. I. Ventre *et al.*, Multiple sensors control reciprocal expression of Pseudomonas aeruginosa regulatory RNA and virulence genes. *Proc. Natl. Acad. Sci. U.S.A.* **103**, 171–176 (2006).
19. X. Latour, The evanescent GacS signal. *Microorganisms* **8**, 1746 (2020).
20. A. Brencic *et al.*, The GacS/GacA signal transduction system of Pseudomonas aeruginosa acts exclusively through its control over the transcription of the RsmY and RsmZ regulatory small RNAs. *Mol. Microbiol.* **73**, 434–445 (2009).
21. K. Lapouge, M. Schubert, F. H. Allain, D. Haas, Gac/Rsm signal transduction pathway of gamma-proteobacteria: From RNA recognition to regulation of social behaviour. *Mol. Microbiol.* **67**, 241–253 (2008).
22. M. Romero *et al.*, Genome-wide mapping of the RNA targets of the Pseudomonas aeruginosa riboregulatory protein RsmN. *Nucleic Acids Res.* **46**, 6823–6840 (2018).
23. A. L. Goodman *et al.*, Direct interaction between sensor kinase proteins mediates acute and chronic disease phenotypes in a bacterial pathogen. *Genes Dev.* **23**, 249–259 (2009).
24. V. I. Francis *et al.*, Multiple communication mechanisms between sensor kinases are crucial for virulence in Pseudomonas aeruginosa. *Nat. Commun.* **9**, 2219 (2018).
25. J. D. Mougous *et al.*, A virulence locus of Pseudomonas aeruginosa encodes a protein secretion apparatus. *Science* **312**, 1526–1530 (2006).
26. G. Xuan, H. Lin, X. Li, J. Kong, J. Wang, RetS regulates phage infection in Pseudomonas aeruginosa via modulating the GacS/GacA two-component system. *J. Virol* **96**, e0019722 (2022), 10.1128/jvi.00197-22.
27. M. Shah *et al.*, A phage-encoded anti-activator inhibits quorum sensing in Pseudomonas aeruginosa. *Mol. Cell* **81**, 571–583.e6 (2021), 10.1016/j.molcel.2020.12.011.
28. D. E. Nivens, D. E. Ohman, J. Williams, M. J. Franklin, Role of alginate and its O acetylation in formation of Pseudomonas aeruginosa microcolonies and biofilms. *J. Bacteriol.* **183**, 1047–1057 (2001).
29. J. P. K. Bravo, C. Aparicio-Maldonado, F. L. Nobrega, S. J. J. Brouns, D. W. Taylor, Structural basis for broad anti-phage immunity by DISARM. *Nat. Commun.* **13**, 2987 (2022).
30. D. Faith *et al.*, Complete genome sequence of the N4-like Pseudomonas aeruginosa bacteriophage vB_PaeP_CMS1. *Microbiol. Resour. Announc.* **11**, e0023922 (2022), 10.1128/mra.00239-22.
31. R. Shigehisa *et al.*, Characterization of Pseudomonas aeruginosa phage KPP21 belonging to family Podoviridae genus N4-like viruses isolated in Japan. *Microbiol. Immunol.* **60**, 64–67 (2016).
32. A. D. Hershey, M. Chase, Independent functions of viral protein and nucleic acid in growth of bacteriophage. *J. Gen. Physiol.* **36**, 39–56 (1952).
33. A. D. Hershey, Some minor components of bacteriophage T2 particles. *Virology* **4**, 237–264 (1957).
34. B. N. Ames, D. T. Dubin, S. M. Rosenthal, Presence of polyamines in certain bacterial viruses. *Science* **127**, 814–815 (1958).
35. B. N. Ames, D. T. Dubin, The role of polyamines in the neutralization of bacteriophage deoxyribonucleic acid. *J. Biol. Chem.* **235**, 769–775 (1960).
36. S. C. Riemer, V. A. Bloomfield, Packaging of DNA in bacteriophage heads: Some considerations on energetics. *Biopolymers* **17**, 785–794 (1978).
37. N. B. Groman, G. Suzuki, Effect of spermine on lysis and reproduction by bacteriophages phi-X174, lambda, and f2. *J. Bacteriol.* **92**, 1735–1740 (1966).
38. H. Reiter, The location of the inhibitory action of Kcn and several polyamines on bacteriophage replication. *Virology* **21**, 636–641 (1963).
39. A. A. Ouameur, H. A. Tajmir-Riahi, Structural analysis of DNA interactions with biogenic polyamines and cobalt(III)hexamine studied by Fourier transform infrared and capillary electrophoresis. *J. Biol. Chem.* **279**, 42041–42054 (2004).
40. A. Osland, K. Kleppe, Influence of polyamines on the activity of DNA polymerase I from Escherichia coli. *Biochim. Biophys. Acta* **520**, 317–330 (1978).

41. M. L. Pato, M. M. Howe, N. P. Higgins, A DNA gyrase-binding site at the center of the bacteriophage Mu genome is required for efficient replicative transposition. *Proc. Natl. Acad. Sci. U.S.A.* **87**, 8716–8720 (1990).
42. A. Brencic, S. Lory, Determination of the regulon and identification of novel mRNA targets of Pseudomonas aeruginosa RsmA. *Mol. Microbiol.* **72**, 612–632 (2009).
43. A. Pingoud *et al.*, Effect of polyamines and basic proteins on cleavage of DNA by restriction endonucleases. *Biochemistry* **23**, 5697–5703 (1984).
44. M. Kuosmanen, H. Poso, Inhibition of the activity of restriction endonucleases by spermidine and spermine. *FEBS Lett.* **179**, 17–20 (1985).
45. P. Plateau, C. Moch, S. Blanquet, Spermidine strongly increases the fidelity of Escherichia coli CRISPR Cas1-Cas2 integrase. *J. Biol. Chem.* **294**, 11311–11322 (2019).
46. S. Meaden *et al.*, Phage gene expression and host responses lead to infection-dependent costs of CRISPR immunity. *Isme J.* **15**, 534–544 (2021).
47. E. R. Westra *et al.*, Parasite exposure drives selective evolution of constitutive versus inducible defense. *Curr. Biol.* **25**, 1043–1049 (2015).
48. J. Wagemans *et al.*, Functional elucidation of antibacterial phage ORFans targeting Pseudomonas aeruginosa. *Cell Microbiol.* **16**, 1822–1835 (2014).
49. J. Wagemans *et al.*, Antibacterial phage ORFans of Pseudomonas aeruginosa phage LUZ24 reveal a novel MvaT inhibiting protein. *Front. Microbiol.* **6**, 1242 (2015).
50. M. Fazli, J. J. Harrison, M. Gambino, M. Givskov, T. Tolker-Nielsen, In-frame and unmarked gene deletions in Burkholderia cenocepacia via an allelic exchange system compatible with gateway technology. *Appl. Environ. Microbiol.* **81**, 3623–3630 (2015).
51. A. K. Schmidt *et al.*, A filamentous bacteriophage protein inhibits type IV Pili to prevent superinfection of Pseudomonas aeruginosa. *mBio* **13**, e0244121 (2022), 10.1128/mbio.02441-21.
52. J. A. Davies *et al.*, The GacS sensor kinase controls phenotypic reversion of small colony variants isolated from biofilms of Pseudomonas aeruginosa PA14. *FEMS Microbiol. Ecol.* **59**, 32–46 (2007).
53. P. R. Secor *et al.*, Filamentous bacteriophage promote biofilm assembly and function. *Cell Host. Microbe* **18**, 549–559 (2015).
54. J. Bondy-Denomy *et al.*, Prophages mediate defense against phage infection through diverse mechanisms. *Isme J.* **10**, 2854–2866 (2016).
55. S. D. Mendoza *et al.*, A bacteriophage nucleus-like compartment shields DNA from CRISPR nucleases. *Nature* **577**, 244–248 (2020).
56. H. P. Schweizer, Escherichia-Pseudomonas shuttle vectors derived from pUC18/19. *Gene* **97**, 109–121 (1991).
57. L. R. Hmelo *et al.*, Precision-engineering the Pseudomonas aeruginosa genome with two-step allelic exchange. *Nat. Protoc.* **10**, 1820–1841 (2015).
58. Y. Liao, G. K. Smyth, W. Shi, The R package Rsubread is easier, faster, cheaper and better for alignment and quantification of RNA sequencing reads. *Nucleic Acids Res.* **47**, e47 (2019).
59. M. D. Robinson, D. J. McCarthy, G. K. Smyth, edgeR: A Bioconductor package for differential expression analysis of digital gene expression data. *Bioinformatics* **26**, 139–140 (2010).
60. H. Mi *et al.*, Protocol Update for large-scale genome and gene function analysis with the PANTHER classification system (v.14.0). *Nat. Protoc.* **14**, 703–721 (2019).
61. J. Kim, A. M. Webb, J. P. Kershner, S. Blaskowski, S. D. Copley, A versatile and highly efficient method for scarless genome editing in Escherichia coli and Salmonella enterica. *BMC Biotechnol.* **14**, 84 (2014).